RESEARCH NOTES

Monodisperse Nanoparticle Synthesis by an Atmospheric Pressure Plasma Process: An Example of a Visible Light Photocatalyst

Hsunling Bai,*,† Chienchih Chen,† Chiahsin Lin,† Walter Den,‡ and Chungliang Chang§

Institute of Environmental Engineering, National Chiao-Tung University, 75 Po-Ai Street, Hsinchu, Taiwan, Department of Environmental Science, Tunghai University, Taichung, Taiwan, and Department of Environmental Engineering and Health, Yuanpei Institute of Science and Technology, Hsinchu, Taiwan

An atmospheric pressure plasma-enhanced nanoparticle synthesis (APPENS) process was proposed to produce a titania-based visible light photocatalyst. The titanium tetraisopropoxide (TTIP) precursor was vaporized with a N_2 carrier gas and entered a nonthermal AC plasma system. The N_2 gas was dissociated into N atoms by the plasma energy, and then they were doped into the precursor vapors. The produced $TiO_{2-x}N_x$ nanoparticles were highly uniform and adjustable in size. The titania-based particle sizes ranged from 25 to 40 nm, and they depended on the precursor ratio of TTIP/H_2O. In addition to producing the photocatalytic particles, the APPENS process has a potential application as a continuous-flow nanosize monodisperse aerosol generator.

1. Introduction

Plasma processes for making powders or films are not new technologies, but they have been operated under either high-temperature or near-vacuum conditions.[1,2] Besides, the product particles by the plasma process were usually broad in size distribution.[3,4] The nonthermal plasma process operated at near-atmospheric pressure and temperature has been successfully applied as commercial ozone generators.[5] Also, its potential application for removing various air pollutants such as volatile organic compounds, nitrogen oxides, and sulfur oxides has been widely studied.[6,7] However, to date, its feasibility to serve as a reactor for nanoparticle or nanofilm production has not yet been studied.

On the other hand, ever since the first paper published concerning its photocatalytic effect,[8] the TiO_2 material has attracted many studies on its potential applications. These include photocatalytic destruction of various environmental pollutants,[9] photocatalytic sterilization, and photocatalytic cancer treatment as well as antifogging and self-cleaning usage due to the photoinduced superhydrophilicity of TiO_2, etc.[10] The anatase TiO_2 nanoparticles have a potential use as solar cell materials also.[11]

Although the application fields may be varied, the size control in the production of TiO_2 nanoparticles has always been an important subject of study. Electrical charges during the gas-phase particle generation process can be used to reduce the average particle size and narrow the size distribution of particles.[12] For example, the unipolarly charged method has been applied to the flame method[13] or the chemical vapor deposition (CVD) method[14] to assist in the production of nonagglomerated nanoparticles.

One of the application limitations for TiO_2 particles as a photocatalysis material is that they utilize only ultraviolet light source. Because TiO_2 absorbs only 2−3% of solar light, modification of the titania particles that utilize a visible light source has been widely studied.[15] Doping of transition metals into TiO_2 particles has been the most common approach to extend their light absorption into the visible region and to reduce recombination of photoregenerated electrons and holes.[16,17] Another promising route is to produce nitrogen-doped TiO_2 particles that enhance the photoactivity in the visible light region. The titania particles can be N-doped via utilization of N_2 gas, ammonium chloride, ammonia gas, or other N-containing bases.[18−23] The N atom can be successfully doped into titania via sputtering of the TiO_2 target in an N_2/Ar gas mixture, and a $TiO_{2-x}N_x$ film was prepared.[19] The substitutional doping of N was the most effective because its p state contributes to the band-gap narrowing by mixing with O 2p states.[19] The $TiO_{2-x}N_x$ film absorbed the light at less than 500-nm wavelength. Recent photocatalytic activity test results confirmed that the $TiO_{2-x}N_x$ nanoparticles are superior to the TiO_2 nanoparticles in the visible light of irradiation.[21−23]

2. Experimental Method

In this study, a continuous-gas-flow reactor was developed to produce $TiO_{2-x}N_x$ nanoparticles with uniform size. The process employs an AC nonthermal plasma operated under atmospheric pressure conditions and is named atmospheric pressure plasma-enhanced nanoparticles synthesis (APPENS) hereafter. The AP-

* To whom correspondence should be addressed. Tel.: 886-3-5731868. Fax: 886-3-5725958. E-mail: hlbai@mail.nctu.edu.tw.

† National Chiao-Tung University.

‡ Tunghai University.

§ Yuanpei Institute of Science and Technology.

10.1021/ie049815x CCC: $27.50
Published on Web 09/25/2004

PENS process has the advantage of operating without the necessity of vacuum conditions, as compared to the radio-frequency plasma process (i.e., the PECVD process). It is operated at atmospheric pressure with low frequency (60 Hz) and thus requires low power. Also, its energy input is still enough to break down the N_2 molecule and thus enables the doping of N atoms into the TiO_2 precursors.

The idea of the APPENS process is very simple. It used titanium tetraisopropoxide [TTIP, $Ti(OC_3H_7)_4$] and H_2O as the precursor materials. They were obtained by passing the N_2 carrier gas into impingers and then mixed, and the resulting solution was fed into the plasma reactor. The reactor was made of Pyrex glass with an inner diameter of 21 mm. The total flow rate of TTIP and H_2O carrier gases was 160 cm^3/min and was controlled by mass flow controllers (Brooks 5860E). The system was operated at an electrical field strength from 0 to 9.6 kV/cm by an ac power supply with 60-Hz frequency. The concentration of the TTIP precursor was controlled by changing either the bath temperature or precursor feed ratio (TTIP/H_2O). The produced particles were heated in a 500 °C oven for 3 h to remove residual carbon.

The photocatalytic reactor for the toluene destruction test was a batch-type reactor. The reactor was made of Pyrex glass with 21 mm i.d., 23 mm o.d., and 200 mm length. The batch reactor was the same one as that for producing the TiO_2 catalytic particles during the APPENS process; that is, the particles were formed and deposited directly on the reactor for later photocatalytic test usage. Blank tests were conducted before the photocatalytic tests. The blank tests included those conducted with a catalyst but without illumination and those without a catalyst but with UV illumination. Both types of blank tests showed that the removal of toluene vapors is negligible.

The illumination light sources of a photocatalytic reactor were UV (365 nm) and visible light (435, 485, and 540 nm). The intensity of both light sources was the same at 10 W. For the batch-type photocatalytic reaction test, a small amount of toluene was injected into the sealed reactor at 45 °C and held for about 60 min to reach a steady-state concentration of 250 ± 10 ppm in the reactor as detected by a gas chromatograph with a flame ionization detector (China Chromotography 9800). Then the light was turned on, and the removal efficiency of the toluene vapor was recorded.

3. Results and Discussion

Because the system was operated without applying atmospheric pressure plasma, polydisperse particles were formed as observed by the scanning electron microscopic (SEM) picture shown in Figure 1a. The particle size range was very broad from nanometer to micron sizes. The micron-sized particles can be either spherical, porous, or doughnut shaped, forming from direct hydrolysis of the TTIP precursor vapors or high agglomeration of primary TiO_2 nanoparticles.

The SEM and transmission electron microscopic (TEM) pictures of particles produced under a plasma environment, i.e., by the APPENS process, are shown in Figure 1b,c. Because the precursor vapors were nucleating to form primary particles, their growth was hindered as a result of the ac applied voltage that produced ions of the same sign at a time. The particles were all charged in either positive or negative sign and

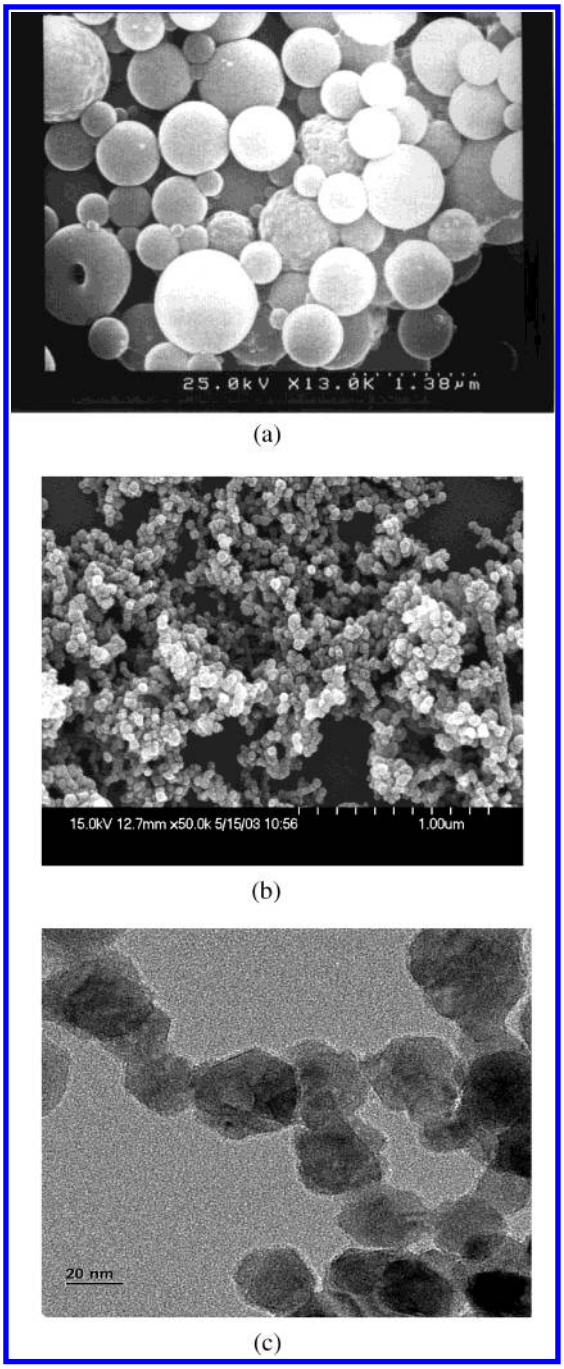

Figure 1. (a) SEM picture of titania-based particles formed without atmospheric pressure plasma. (b and c) SEM and TEM pictures of titania-based particles formed with applying atmospheric pressure plasma.

repelled each other. Besides, the local thermal equilibrium plasma under ac provides a near-neutral environment; thus, a neutralizer may not be required after the nonthermal plasma reactor.

The SEM and TEM pictures of particles revealed that a change in the precursor bath temperature from 100 to 175 °C did not change the size of the product particles. Similarly, collecting particles at different locations of the reactor showed that a change in the plasma residence time from 1 to 17 s did not change the particle size. However, an increase in the TTIP/H_2O precursor ratio resulted in an increase in the particle size. For the present study, the photocatalytic particles with size ranging from 20 to 40 nm are achievable for TTIP/H_2O ratios of 0.125:4. This falls in the size range that had

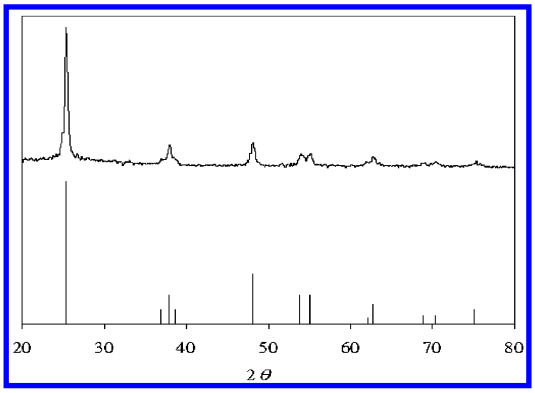

Figure 2. Titania-based nanoparticle characterized by XRPD (upper plot) and compared to the JCPDS file (bottom plot) of anatase TiO_2.

been confirmed to be optimal for photooxidation of organic substrates in water.[24]

To confirm the monodispersity, the TTIP precursor flow was further diluted to prevent loose agglomeration of particles at high concentration, and then the size distribution was determined by the scanning mobility particle sizer (SMPS; TSI model 3080L). The geometric standard deviations of the particle size distribution were found to be around 1.10 ± 0.03 at particle concentrations below 10^6 cm^{-3}. As suggested in the literature,[1] a σ_g of less than 1.2 is monodisperse and a σ_g of less than 1.0 is highly monodisperse. Also, with a σ_g of 1.10, about 95% of the particles fall within size ranges of 16−24, 25−36, and 33−48 nm respectively for average diameters of 20, 30, and 40 nm.[25] Thus, we can say that monodisperse nanoparticles can be continuously generated by the APPENS process proposed in this study.

The titania-based product particles for the APPENS process were characterized by X-ray powder diffraction (XRPD), and the result is shown in Figure 2. As compared to the JCPD file, the peaks of product particles were confirmed to be in the anatase form. Surface analyses of particles were detected by both energy-dispersive spectrometry (EDS) and electron spectroscopy for chemical analysis (ESCA) to identify whether the product particles contain N atoms. Both revealed that Ti, O, and N atoms were found in the product particles. From the EDS analysis, one observed that most of the product particles were composed of Ti and O atoms; only a slight amount of N atoms was found. The atomic concentration of N is 1.25% in the N-containing TiO_2 catalysts as analyzed by ESCA. The N-containing TiO_2 particles were manufactured at an electric intensity of 10.8 kV/cm and a TTIP/H_2O molar ratio of 4.0. As the operation condition was varied, the atomic concentration of N would vary.

Figure 3 shows the ESCA for confirming the presence of $TiO_{2-x}N_x$. As obtained from the ESCA data bank, the peak binding energy for Ti $2p_{3/2}$ and Ti $2p_{1/2}$ in TiO_2 should be around 458.8 and 464.3 eV, respectively. Our binding energy data have slightly different peak values of Ti 2p at 459.3 and 464.9 eV, respectively, as shown in the upper plot of Figure 3. Although the slight differences in the binding energy values are within the error range of ESCA, they could also be due to the N-doping effect that leads to shifts on the binding energy values of Ti 2p.[26] The N-doping effect is more clearly seen by the presence of nitride around 396−398 eV, as shown in the bottom plot of Figure 3. Hence, results of the analyses together with literature information[22,23] indicated that the catalyst particles produced in this study have the structure of $TiO_{2-x}N_x$.

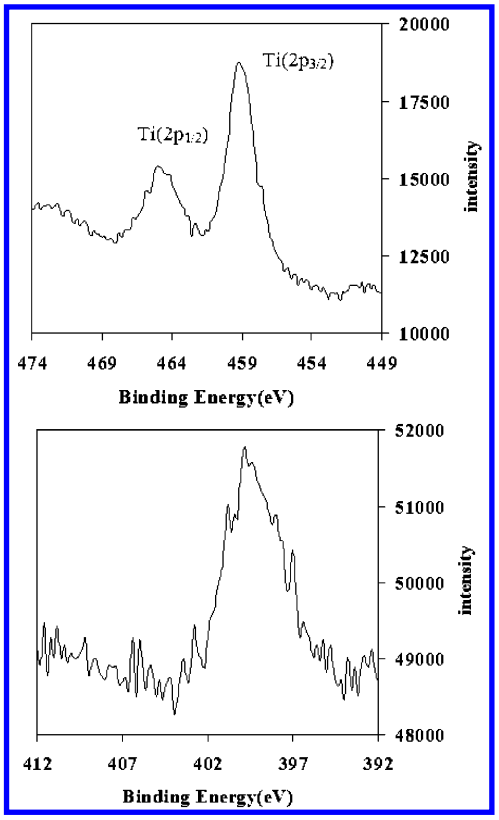

Figure 3. Evidence of Ti (upper plot) and N 1s (bottom plot) in TiO_2 as analyzed by the ESCA that shows the presence of the $TiO_{2-x}N_x$ structure of the product particles.

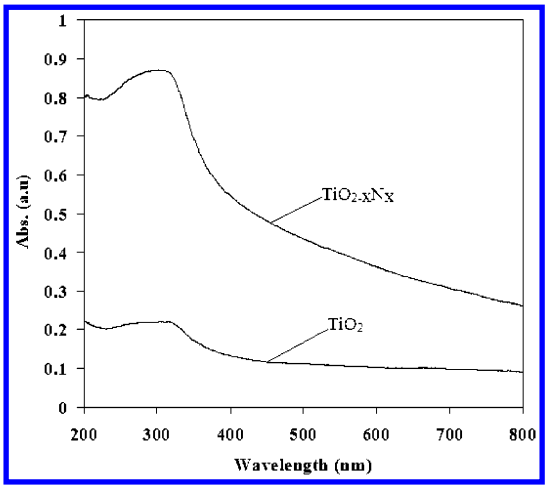

Figure 4. Absorption spectra of TiO_2 (obtained by air plasma) and $TiO_{2-x}N_x$ (obtained by N_2 plasma).

Photocatalytic particles of both pure TiO_2 and N-containing TiO_2 were prepared as 100 mg/L aqueous solutions and were tested by a photospectrometer (Shimadzu UV-2501PC) for its absorption spectrum. Although we are not able to measure the band gap of the $TiO_{2-x}N_x$ particles at the present time, however, it is known that the band gap of N-doped TiO_2 is slightly narrowed by about 0.01−0.05 eV as compared to the band gap of pure TiO_2, 3.16 eV.[21] As seen in Figure 4, the slight narrowing in the band gap leads to increases in the absorption intensity in both visible and UV light ranges.

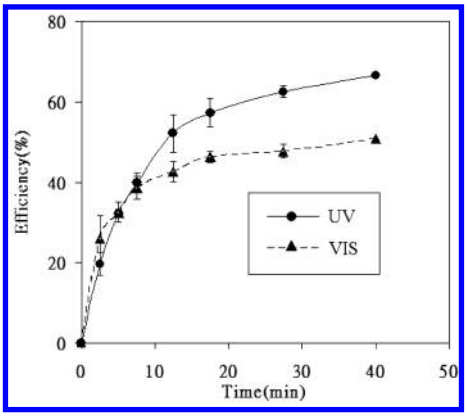

Figure 5. Batch experimental results of toluene decomposition efficiencies under UV (10 W and 365 nm) and visible (10 W and 435, 485, and 540 nm) light ranges.

The results of toluene removal tests are shown in Figure 5. One can see that the N-doped titania-based particles are photoactive under both UV and visible light sources. The differences in the decomposition rates between the UV and visible light illumination at the beginning of the irradiation were within experimental errors. That is, they have a similar decomposition rate at the very beginning of the irradiation. Also, after 10 min of irradiation, the decomposition rate is slower for the visible light irradiation than that for the UV light irradiation. This may be because the absorption intensity is still stronger in the UV light range than it is in the visible light range, as shown by the absorption spectra in Figure 4. So, at the same light intensity of 10 W, the utilization of light energy was lower for visible light and resulted in a slower decomposition rate. Similar observations have also been seen in the literature.[19,22]

4. Conclusion

In addition to the application of the APPENS process to the production of photocatalyst in the nanometer-size range, it has a potential application to serve as a continuous-flow monodisperse nanoparticle generator. For monodisperse particle generation purposes, it is readily applicable with roughly the same design as indicated in this study, while to serve as a photocatalytic nanoparticle production process, the reactor design with parallel-tube geometry is necessary to enlarge its production rate.[7]

Acknowledgment

This study was supported by the National Science Council, Taiwan, through Grants NSC 91-2211-E-009-012 and NSC 92-2211-E-009-017. Assistance from Dr. H. M. Chien, Dr. Y. D. Hsu, and Z. M. Chen from ITRI, Taiwan, in conducting the SMPS analysis is greatly appreciated.

Literature Cited

(1) Kodas, T. T.; Hampden-Smith, M. J. *Aerosol Processing of Materials*; Wiley-VCH: New York, 1999.

(2) Fujimoto, T.; Okuyama, K.; Shimada, M.; Fujishige, Y.; Adachi, M.; Matsui, I. *J. Appl. Phys.* **2000**, *88*, 3047.

(3) Pratsinis, S. E.; Kodas, T. T. Manufacturing of Materials by Aerosol Processes. In *Aerosol Measurement*; Willeke, K., Baron, P. A., Eds.; Van Nostrand Reinhold: New York, 1993.

(4) Friedlander, S. K. *Smoke, Dust and Haze: Fundamentals of Aerosol Dynamics*, 2nd ed.; Oxford University Press: New York, 2000.

(5) Chang, M. B.; Wu, S. J. *Ozone: Sci. Eng.* **1997**, *19*, 241.

(6) Chang, M. B.; Chang, C. C. *AIChE J.* **1997**, *43*, 1325.

(7) Lin, C.-H.; Bai, H. *ASCE J. Environ. Eng.* **2001**, July, 648.

(8) Fujishima, A.; Honda, K. *Nature* **1972**, *238*, 37.

(9) Zhao, J.; Yang, X. *Build. Environ.* **2003**, *38*, 645.

(10) Fujishima, A.; Rao, T. N.; Tryk, D. A. *J. Photochem. Photobiol. C* **2000**, *1*, 1.

(11) Nakade, S.; Saito, Y.; Kubo, W.; Kitamura, T.; Wada, Y.; Yanagida, S. *J. Phys. Chem. B* **2003**, *107*, 8607.

(12) Xiong, Y.; Pratsinis, S. E.; Mastrangelo, S. V. R. *J. Colloid Interface Sci.* **1992**, *153*, 106.

(13) Kammler, H. K.; Jossen, R.; Morrison, P. W.; Pratsinis, S. E.; Beaucage, G. *Powder Technol.* **2003**, Sp. Iss. SI, *135*, 310.

(14) Nakaso, K.; Han, B.; Ahn, K. H.; Choi, M.; Okuyama, K. *J. Aerosol Sci.* **2003**, *34*, 869.

(15) Anpo, M.; Takeuchi, M. *J. Catal.* **2003**, *216*, 505.

(16) Choi, W.; Termin, A.; Hoffmann, M. R. *J. Phys. Chem.* **1994**, *98*, 13669.

(17) Yuan, Z. H.; Jia, J. H.; Zhang, L. D. *Mater. Chem. Phys.* **2002**, *73*, 323.

(18) Sato, S. *Chem. Phys. Lett.* **1986**, *123*, 126.

(19) Asahi, R.; Morikawa, T.; Ohwaki, T.; Aoki, K.; Taga, Y. *Science* **2001**, *293*, 269.

(20) Ihara, T.; Miyoshi, M.; Iriyama, Y.; Matsumoto, M.; Sugihara, S. *Appl. Catal. B* **2003**, *42*, 403.

(21) Sakthivel, S.; Kisch, H. *ChemPhysChem* **2003**, *4*, 487 (www.chemphyschem.org).

(22) Irie, H.; Watanabe, Y.; Hashimoto, K. *J. Phys. Chem. B* **2003**, *107*, 5483.

(23) Burda, C.; Lou, Y.; Chen, X.; Samia, A. C. S.; Stout, J.; Gole, J. L. *Nano Lett.* **2003**, *3*, 1049.

(24) Almquist, C. B.; Biswas, P. *J. Catal.* **2002**, *212*, 145.

(25) Hinds, W. C. *Aerosol Technology*, 2nd ed.; John Wiley and Sons: New York, 1999.

(26) Zheng, S.; Li, Z.; Gao, L. *Mater. Chem. Phys.* **2004**, *85*, 195.

Received for review March 7, 2004
Revised manuscript received July 1, 2004
Accepted July 21, 2004

IE049815X